



Contents lists available at ScienceDirect

## Bioorganic &amp; Medicinal Chemistry Letters

journal homepage: [www.elsevier.com/locate/bmcl](http://www.elsevier.com/locate/bmcl)Discovery of imidazo[1,2-*a*]pyrazine-based Aurora kinase inhibitorsDavid B. Belanger<sup>a,\*</sup>, Patrick J. Curran<sup>a</sup>, Alan Hruza<sup>b</sup>, Johannes Voigt<sup>b</sup>, Zhaoyang Meng<sup>a</sup>, Amit K. Mandal<sup>a</sup>, M. Arshad Siddiqui<sup>a</sup>, Andrea D. Basso<sup>c</sup>, Kimberly Gray<sup>c</sup><sup>a</sup> Department of Chemistry, Merck Research Laboratories, 320 Bent Street, Cambridge, MA 02141, United States<sup>b</sup> Department of Chemistry, Merck Research Laboratories, 2015 Galloping Hill Road, Kenilworth, NJ 07033, United States<sup>c</sup> Department of Oncology, Merck Research Laboratories, 2015 Galloping Hill Road, Kenilworth, NJ 07033, United States

## ARTICLE INFO

## Article history:

Received 20 May 2010

Revised 1 July 2010

Accepted 2 July 2010

Available online 8 July 2010

## Keywords:

Aurora kinase inhibitors

Imidazo[1,2-*a*]pyrazine

## ABSTRACT

The synthesis and structure–activity relationships (SAR) of novel, potent imidazo[1,2-*a*]pyrazine-based Aurora kinase inhibitors are described. The X-ray crystal structure of imidazo[1,2-*a*]pyrazine Aurora inhibitor **1j** is disclosed. Compound **10i** was identified as lead compound with a promising overall profile.

© 2010 Elsevier Ltd. All rights reserved.

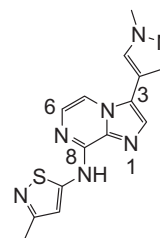
Aurora kinases A, B, and C are cell cycle regulated serine/threonine kinases expressed only during mitosis.<sup>1</sup> Ubiquitously expressed Aurora A regulates cell cycle events such as centromere maturation, bipolar spindle assembly, mitotic entry and exit, as well as, kinetochore–spindle attachment.<sup>1</sup> Aurora B phosphorylates histone H3, regulates chromosomal remodeling, kinetochore–spindle attachment, and cytokinesis.<sup>1</sup> Aurora C is believed to have a function related to Aurora B but has limited expression.<sup>1</sup> Aurora A and B are essential protein kinases and as such are required for successful mitotic progression. siRNA depletion of Aurora A results in G2/M delay followed by apoptotic cell death. siRNA depletion of Aurora B causes aberrant endoreduplication (polyploidy) followed by apoptosis. Dual Aurora A/B siRNA knockdown displays an Aurora B siRNA phenotype.<sup>1</sup> Since it was first discovered that Aurora A kinase was over expressed in breast tumors,<sup>2</sup> intense academic, and pharmaceutical research has helped develop a better understanding of the role of Aurora kinases in cancer. Amplification or over expression of Aurora kinases has been observed in multiple tumor types<sup>3,4</sup> and is often correlated with poor prognosis.<sup>5</sup>

According to recent letters, 13 Aurora inhibitors are currently in Phase I/II clinical trials with many other companies in preclinical research.<sup>4,6</sup> Interestingly, a diverse set of Aurora kinase inhibitors has progressed to clinical trials (selective Aurora A, selective Aurora B, or Aurora A/B inhibitors), yet no drugs have been approved for use. Our initial goal was to identify an Aurora A/B kinase inhibitor with sub-micromolar target engagement (phos-HH3) and an in vitro DMPK profile suitable for progression to lead optimization.

Herein, we report our initial SAR findings in the imidazo[1,2-*a*]pyrazine series and the first X-ray structure of this compound class with Aurora A.

Screening of our internal compound library against Aurora A identified imidazo[1,2-*a*]pyrazine-based inhibitors (Fig. 1).<sup>14</sup> Compound **1** was a low molecular weight (MW = 311.37), modestly potent Aurora A and Aurora B inhibitor (Aurora A IC<sub>50</sub> = 0.57 μM, Aurora B IC<sub>50</sub> = 0.36 μM). Our primary objective was to improve biochemical potency and mechanism-based cell activity (phos-HH3). Medicinal chemistry efforts commenced by simultaneously investigating the SARs at the 3-, 6- and 8-positions.

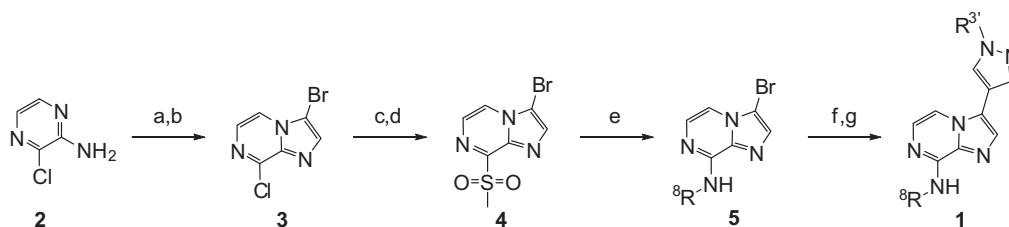
The synthetic route to 3-, 8-disubstituted imidazo[1,2-*a*]pyrazine analogs of Aurora inhibitor **1** is shown in Scheme 1. The imidazo[1,2-*a*]pyrazine core structure was assembled by condensation of chloroacetaldehyde and commercially available 2-amino-3-chloropyrazine **2**.<sup>7</sup> Subsequent bromination with bromine in acetic acid afforded the 3-bromo-8-chloroimidazo[1,2-*a*]pyrazine **3** in



Aurora A IC<sub>50</sub> = 0.57 μM  
Aurora B IC<sub>50</sub> = 0.36 μM

Figure 1. Aurora kinase screening hit **1**.

\* Corresponding author. Tel.: +1 617 499 3504; fax: +1 617 499 3535.  
E-mail address: [david.belanger@merck.com](mailto:david.belanger@merck.com) (D.B. Belanger).



**Scheme 1.** Reagents and conditions: (a) 2-chloroacetaldehyde diethyl acetal, concd HCl, water, reflux; Et<sub>2</sub>O extract, concentrate, 2-amino-3-chloropyrazine, cat. HCl, DME, reflux, 90%; (b) AcOH, Br<sub>2</sub>, rt, 91%; (c) NaSMe, MeOH, rt, 95%; (d) *m*-CPBA, DCM, rt, 95%; (e) NaH, DMSO, aniline, rt; (f) Suzuki reaction; (g) 4 N HCl dioxane, if necessary.

**Table 1**  
Aurora A inhibition data for imidazopyrazines **1a–l**

Compd	R <sup>8</sup>	R <sup>3'</sup>	Aurora A <sup>a</sup> IC <sub>50</sub> (μM)	Aurora B <sup>a</sup> IC <sub>50</sub> (μM)
<b>1a</b>		Me	0.57	0.26
<b>1b</b>		Me	0.64	0.70
<b>1c</b>		Me	1.6	0.20
<b>1d</b>		Me	0.17	0.11
<b>1e</b>		Me	>10	N/A
<b>1f</b>		Me	>10	N/A
<b>1g</b>		Me	2.5	3.0
<b>1h</b>		Me	>10	N/A
<b>1i</b>		Me	3.7	N/A
<b>1j</b>		H	≤0.004	≤0.013

**Table 1** (continued)

Compd	R <sup>8</sup>	R <sup>3'</sup>	Aurora A <sup>a</sup> IC <sub>50</sub> (μM)	Aurora B <sup>a</sup> IC <sub>50</sub> (μM)
<b>1k</b>		H	0.006	0.018
<b>1l</b>		H	0.081	0.12

<sup>a</sup> Assay conditions listed in Ref. 15.

good yield. Intermediate **3** was originally envisioned to be a vital synthetic intermediate as we<sup>8</sup> and others<sup>9</sup> had shown that various amines and anilines could be added to the 8-position. In our hands, the reaction of dihalide **3** with anilines (e.g., 3-dimethylamino aniline) proceeded quite sluggishly even using forcing conditions (excess aniline, reaction temperature >150 °C). Furthermore, less nucleophilic aminoheterocycles (e.g., 2-amino-5-methylthiazole) failed to give any product. Auspiciously, we found that 3-bromo-8-(methylsulfonyl)imidazo[1,2-*a*]pyrazine **4** was quite reactive toward various anilines and aminoheterocycles such as 2-amino-5-methylthiazole. Sulfone **4** was prepared in two steps by sequential treatment of 3-bromo-8-chloroimidazo[1,2-*a*]pyrazine **3** with sodium methanethiolate followed by *m*-chloroperbenzoic acid oxidation.<sup>10</sup> Installation of groups at the 3-position was achieved by a Suzuki reaction.

Initial SAR studies revealed that only isothiazole analogs related to hit **1a** retained Aurora A potency (Table 1, compounds **1b–d**). Structurally similar congeners derived from 8-aminothiadiazole **1e** and 8-aminothiazole **1f** were found to be significantly less active than the initial screening hit **1a**. Interestingly, 8-aminothiophene analog **1g** retained modest potency versus Aurora A, but most substituted anilines showed enzyme potency >5 μM. The distinct preference for precise 8-position sulfur containing heterocycle was clearly evident given that over 50 substituted aniline analogs of **1a** were evaluated and all showed poor biochemical potency (Aurora A IC<sub>50</sub> >5 μM). In contrast, Aurora A was more receptive to inhibitors bearing an unsubstituted 3-(4-pyrazolo) group. For instance, isothiazole inhibitors **1j** and **1k** both showed improved enzyme potency (Aurora A IC<sub>50</sub> ≤ 4 nM and 6 nM, respectively) and low micromolar target engagement (phos-HH3 IC<sub>50</sub> = 1.3 μM). Furthermore, inclusion of the 3-(4-pyrazolo) afforded inhibitors (e.g., 8-aniline **1l**) with improved Aurora A potency though sulfur containing heterocycles were still preferred.

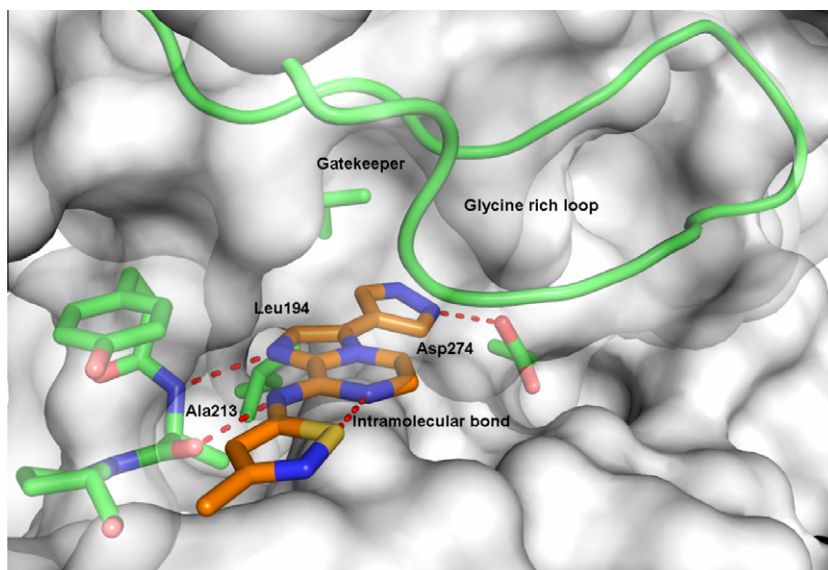
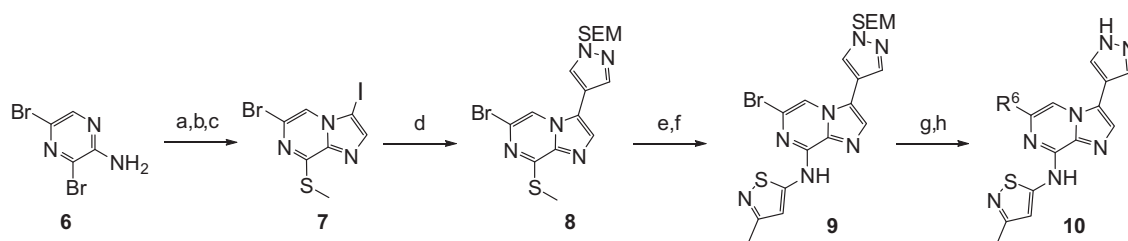


Figure 2. X-ray structure of inhibitor **1j** in Aurora A (2.4 Å). Graphic was prepared using PyMOL.<sup>16</sup>



Scheme 2. Reagents and conditions: (a) 50% chloroacetaldehyde in water, IPA, *relux*, 89%; (b) NaSMe, MeOH, *rt*, 95%; (c) *N*-iodosuccinimide, DMF, 60 °C, 76%; (d) 5 mol % PdCl<sub>2</sub>(dppf), K<sub>3</sub>PO<sub>4</sub>, 1,4-dioxane/water (10/1), 40 °C, 46%; (e) *m*-CPBA, DCM, *rt*, 95%; (f) NaH, 5-amino-3-methyl isothiazole hydrochloride, DMSO, *rt*, 56%; (g) chemistry varies; (h) 4 N HCl dioxane in THF.

The X-ray crystal structure of inhibitor **1j** in Aurora A revealed the inhibitor **1j** binds in the adenosine triphosphate (ATP) pocket (Fig. 2).<sup>11</sup> The imidazo[1,2-*a*]pyrazine core forms key donor–acceptor hydrogen bonds to the main chain carbonyl oxygen and amide NH of Ala213. The ATP competitive inhibitor projected the 3-(4-pyrazolo) group toward Asp274 with the Aurora A in the catalytically active ‘DFG-in’ conformation.<sup>12</sup> Additionally, the hydrophobic pocket formed between the imidazo[1,2-*a*]pyrazine core and 3-(4-pyrazolo) allows the side chain of Leu194 to pack next to the inhibitor. The noteworthy potency disparity between *N*-methyl pyrazole analog **1a** and the *N*-H pyrazole inhibitor **1j** was attributed primarily to the stabilizing hydrogen bond with Asp274 and to removal of a putative repulsive van der Waals interaction between the Asp274 and *N*-methyl group of inhibitor **1a**.<sup>13</sup> The X-ray also revealed the 8-aminoisothiazole group was located entirely within a hydrophobic region at the front of the ATP binding pocket and extended toward the solvent accessible front. Presumably, the preferred bioactive conformation of the 8-aminoisothiazole and the imidazo[1,2-*a*]pyrazine core in potent inhibitor **1j** was stabilized through a polar interaction between the core nitrogen the isothiazole sulfur atom.<sup>14</sup>

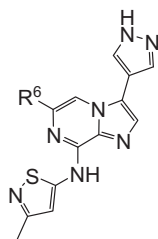
In order to more thoroughly investigate the imidazo[1,2-*a*]pyrazine SAR, a synthetic route was developed that enabled elaboration of the 6-position.<sup>13</sup> 2-Amino-3,5-dibromopyrazine **6** was converted to 6-bromo-3-(4-pyrazolo)-8-aminoisothiazoleimidazo[1,2-*a*]pyrazine **9** using the sequence depicted in Scheme 2. The key step in the sequence was a chemoselective Suzuki reaction of 3-iodo-6-bromoimidazo[1,2-*a*]pyrazine **7** that afforded SEM-

protected pyrazole **8** in acceptable yield. The two step sequence from 6-bromide **8** gave intermediate **9** (*m*-CPBA, then NaH, 5-amino-3-methyl isothiazole hydrochloride).

With the crucial intermediate **9** in hand, Pd-mediated functionalization was used to install different 6-position groups (Table 2). The SAR showed that small, hydrophobic groups were tolerated and preferred (e.g., 6-Me **10a**, 6-Et **10d**, 6-SMe **10i**) over larger groups (e.g., 6-(3-pyridyl) **10h**), 6-cyclopropyl **10f**, 6-*S*-*t*-Bu **10n**). Substituents bearing polar (**10j**, **10k**, and **10p**) or basic functionality (**10b**, **10e**, and **10m**) showed significantly less biochemical potency than the parent compound **1j**. Inhibitors **10a** (6-Me) and **10i** (6-SMe) consistently showed better cell based potency than parent compound **1j**. Inhibitor **10i** demonstrated mechanism-based cell activity with an EC<sub>50</sub> of 0.6 μM. Consistent with the expected phenotype of a pan Aurora inhibitor, at this dose **10i** decreased phosphorylation of Histone H3 and induced >4 N DNA content as measured by FACS. Inhibitor **10i** also potently inhibited tumor cell line growth in a panel of cells from different tissue origin and genetic backgrounds (e.g., p53, PTEN, etc.).

With the identification of Aurora inhibitors with sub-micromolar cell based potency, *in vitro* DMPK properties were evaluated. Inhibitor **10i** showed a good CYP inhibition profile (3A4, 2D6, and 2C9 >20 μM), displayed a modest hERG signal (8.7% Rb efflux<sup>17</sup> at 1.5 μg/mL) and showed high human plasma protein binding (99.4%). Inhibitor **10i** had good measured permeability (Caco-2 apical to basolateral = 633 nm/s, efflux ratio = 1.0), but suffered from high *in vitro* hepatocyte clearance (human = 49.7 μL/min/million cells). The oral bioavailability of **10i** in mouse was low (%F = 4)

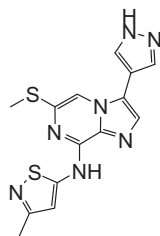
**Table 2**  
Aurora A and B inhibition data for imidazopyrazines **1j–10p**



Compd	R6	Aurora A <sup>a</sup> IC <sub>50</sub> (nM)	Aurora B <sup>a</sup> IC <sub>50</sub> (nM)	phos-HH3 <sup>a</sup> EC <sub>50</sub> (μM)
<b>1j</b>	H	≤4	≤13	1.3
<b>10a</b>	Me	≤4	≤13	0.25
<b>10b</b>	CH <sub>2</sub> morpholine	50	110	>10
<b>10c</b>	CF <sub>3</sub>	27	252	>10
<b>10d</b>	Et	≤4	≤13	0.85
<b>10e</b>	CH <sub>2</sub> CH <sub>2</sub> NH <sub>2</sub>	83	33	>10
<b>10f</b>	CycloPr	17	51	2.6
<b>10g</b>	CN	46	219	>10
<b>10h</b>	3-Pyridyl	8	62	>10
<b>10i</b>	SMe	≤4	≤13	0.6
<b>10j</b>	(±)-S(O)Me	30	185	>10
<b>10k</b>	SO <sub>2</sub> Me	603	>3000	not tested
<b>10l</b>	SEt	22	24	3.0
<b>10m</b>	SCH <sub>2</sub> CH <sub>2</sub> NMe <sub>2</sub>	82	81	>10
<b>10n</b>	S- <i>t</i> -Bu	105	272	5.6
<b>10o</b>	S-4-Fluorophenyl	85	129	2.5
<b>10p</b>	N-Pyrrolidinone	14	26	9.5

<sup>a</sup> Assay conditions listed in Ref. 15.

**Table 3**  
Kinase inhibition profile of Aurora inhibitor **10i**



Kinase	IC <sub>50</sub> (nM)	Kinase	IC <sub>50</sub> (nM)
Aurora A	≤4	IRAK4	167
Aurora B	≤13	Jak2	>10,000
Akt1	>10,000	LCK	468
Camk4	>10,000	cMet	>10,000
Cdk2	2273	MST2	>10,000
Chk1	187	PKCa	>10,000
CSNK1d	1900	PLK3	785
EGFR	5048	Rock2	>10,000
Erk2	>10,000	RSK2	1306
IGRF	>10,000	TSSK2	>10,000
IKKb	>10,000	VEGFR2	36

presumably due to low aqueous solubility (25 μM) and high first pass metabolism (Cl = 89 mL/min/kg). The kinase inhibition profile of compound **10i** is shown in Table 3. Compound **10i** is a potent inhibitor of Aurora A and B (Aurora A TdF = 0.2 nM, Aurora B TdF = 0.4 nM) without inhibiting a number of other kinases (e.g., Akt1, ERK2, JAK2). However, sub-micromolar kinase activity was observed against Chk1, IRAK4, LCK, PLK3, and VEGFR2.

In summary, we have discovered imidazo[1,2-*a*]pyrazine Aurora kinase inhibitors with sub-micromolar on-target cell based activity and a promising overall profile. The initial SAR suggests

the preference for an unsubstituted pyrazole and aminoisothiazole at the 3- and 8-positions, respectively. An X-ray structure has enabled the understanding of the inhibitor binding mode and helped us identify opportunities for improving the characteristics (solubility, in vitro hepatocyte clearance) of these early lead compounds. Future publications from our group will detail the optimization of the imidazo[1,2-*a*]pyrazine series.

#### Acknowledgments

We thank Drs. John Piwinski, Neng-Yang Shih, Paul Kirschmeier, and W. Robert Bishop for support of this work. We also thank Dr. Jayaram Tagat for the preparation of compound **10b**.

#### References and notes

- (a) Andrews, P. D. *Oncogene* **2005**, *24*, 5005; (b) Pollard, J. R.; Mortimore, M. J. *Med. Chem.* **2009**, *52*, 2629; (c) Carpinelli, P.; Moll, J. *Expert Opin. Ther. Targets* **2008**, *12*, 69.
- Tanaka, T.; Kimura, M.; Matsunaga, K.; Fukada, D.; Mori, H.; Okano, Y. *Cancer Res.* **1999**, *59*, 2041.
- (a) Dar, A. A.; Zaika, A.; Piazuolo, M. B.; Correa, P.; Koyama, T.; Belkhir, A.; Washington, K.; Castells, A.; Pera, M.; El-Rifai, W. *Cancer* **2008**, *112*, 1688; (b) Wang, X. X.; Liu, R.; Jin, S. Q.; Fan, F. Y.; Zhan, Q. M. *Cell Res.* **2006**, *16*, 356; (c) Ullisse, S.; Delcros, J. G.; Baldini, E.; Toller, M.; Curcio, F.; Giacomelli, L.; Prigent, C.; Ambesi-Impiombato, F. S.; D'Armiento, M.; Arlot-Bonnemains, Y. *Int. J. Cancer* **2006**, *119*, 275; (d) Ikezoe, T.; Yang, J.; Nishioka, C.; Tasaka, T.; Taniguchi, A.; Kuwayama, Y.; Komatsu, N.; Bandobashi, K.; Togitani, K.; Koeffler, H. P.; Taguchi, H. *Mol. Cancer Ther.* **2007**, *6*, 1851.
- Cheung, C. H.; Coumar, M. S.; Hsieh, H. P.; Chang, J. Y.; Coumar, M. S.; Cheung, C. H.; Chang, J. Y.; Hsieh, H. P. *Expert Opin. Investig. Drugs* **2009**, *18*, 379.
- (a) Tanaka, E.; Hashimoto, Y.; Ito, T.; Okumura, T.; Kan, T.; Watanabe, G.; Imamura, M.; Inazawa, J.; Shimada, Y. *Clin. Cancer Res.* **2005**, *11*, 1827; (b) Kurai, M.; Shiozawa, T.; Shih, H. C.; Miyamoto, T.; Feng, Y. Z.; Kashima, H.; Suzuki, A.; Konishi, I. *Hum. Pathol.* **2005**, *36*, 1281.
- Coumar, M. S.; Cheung, C. H.; Chang, J. Y.; Hsieh, H. P. *Expert Opin. Ther. Patents* **2009**, *19*, 321.
- We found that higher yields were achieved by using chloroacetaldehyde freshly prepared from the corresponding diethylacetal rather than using commercially available aqueous chloroacetaldehyde.
- Guzi, T.; Paruch, K.; Dwyer, M.; Zhao, L.; Curran, P. J.; Belanger, D. B.; Hamann, B.; Reddy, P. A.; Siddiqui, M. A. U.S. 2006/106023 (A1).

9. Sun, C. L.; Liang, C.; Huang, P.; Harris, G. D.; Guan, H. US/2004/0220189; Sun, C. L.; Liang, C.; Huang, P.; Harris, G. D.; Guan, H. US/2005/009832.
10. 3-Bromo-8-(methylsulfonyl)imidazo[1,2-a]pyrazine **4** is a stable solid that can be stored cold for months without decomposition.
11. The coordinates for compound **1j** have been deposited in the RCSB Protein Data Bank under the Accession Code 3NRM.
12. (a) Nowakowski, J.; Cronin, C. N.; McRee, D. E.; Knuth, M. W.; Nelson, C. G.; Pavletich, N. P.; Rogers, J.; Sang, B.-C.; Scheibe, D. N.; Swanson, R. V.; Thompson, D. A. *Structure* **2002**, *10*, 1659; (b) Zuccotto, F.; Ardini, E.; Casale, E.; Angiolini, M. *J. Med. Chem.* **2009**, *53*, 2681; (c) Morphy, R. *J. Med. Chem.* **2010**, *53*, 1413.
13. Subsequent X-ray data with related imidazo[1,2-a]pyrazine inhibitors revealed a water mediated hydrogen bond between the enzyme and the 3-(4-pyrazolo) group. Yu, T.; Tagat, J. R.; Kerekes, A. D.; Doll, R. J.; Zhang, Y.; Xiao, Y.; Esposito, S.; Belanger, D. B.; Curran, P. J.; Amit K. Mandal; Siddiqui, M. A.; Shih, N.-Y.; Basso, A. D.; Liu, M.; Gray, K.; Tevar, S.; Jones, J.; Lee, S.; Ponery, S.; Smith, E. B.; Hruza, A.; Voigt, J.; Ramanathan, L.; Prosser, W.; Hu, M. *J. Med. Chem. Lett.* **2010**, <http://pubs.acs.org/doi/abs/10.1021/ml100063w>.
14. The conformational preference of thiazoles in related systems has been documented. (a) Pierce, A. C.; ter Haar, E.; Binch, H. M.; Kay, D. P.; Patel, S. R.; Li, P. *J. Med. Chem.* **2005**, *48*, 1278; (b) Jung, F. H.; Pasquet, G.; Lambert-van der Brempt, C.; Lohmann, J. J.; Warin, N.; Renaud, F.; Germain, H.; De Savi, C.; Roberts, N.; Johnson, T.; Dousson, C.; Hill, G. B.; Mortlock, A. A.; Heron, N.; Wilkinson, R. W.; Wedge, S. R.; Heaton, S. P.; Odedra, R.; Keen, N. J.; Green, S.; Brown, E.; Thompson, K.; Brightwell, S. *J. Med. Chem.* **2006**, *49*, 955.
15. *Biochemical assays:* Aurora A and B kinase assays were performed in low protein binding 384-well plates. Compounds were diluted in 100% DMSO to the desired concentrations. For the Aurora A assay, each reaction consisted of 8 nM enzyme (Aurora A, Upstate), 100 nM Tamra-PKAtide (Molecular Devices, 5TAMRA-GRTGRRNSICOOH), 25  $\mu$ M ATP, 1 mM DTT, and kinase buffer (10 mM Tris, 10 mM MgCl<sub>2</sub>, 0.01% Tween 20). For the high throughput screen the Aurora A assay was modified and utilized 4 nM enzyme, 100 nM PKAtide, and 100  $\mu$ M ATP. For the Aurora B assay, each reaction consisted of 26 nM enzyme (Aurora B, Invitrogen), 100 nM Tamra-PKAtide (Molecular Devices, 5TAMRA-GRTGRRNSICOOH), 50  $\mu$ M ATP, 1 mM DTT, and kinase buffer (10 mM Tris, 10 mM MgCl<sub>2</sub>, 0.01% Tween 20). Dose–response curves were plotted from inhibition data generated in duplicate, from eight point serial dilutions of inhibitory compounds. Concentration of compound was plotted against kinase activity, calculated by degree of fluorescent polarization. To generate IC<sub>50</sub> values, the dose–response curves were then fitted to a standard sigmoidal curve and IC<sub>50</sub> values were derived by nonlinear regression analysis. *Immunofluorescent assays:* HCT-116 cells were plated at 15,000 cells per well in poly-D-lysine coated black micro-clear 384-well tissue culture plates. For the phos-Histone H3 assay, cells were first treated with 0.4 mg/mL nocodazole. Sixteen hours later cells were treated in triplicate with compound (0.1% final DMSO concentration) for 1 h. Cells were fixed with Prefer<sup>®</sup> fixation solution (Anatech) plus 1000 nM Hoechst 33342 dye and incubated for 30 min at room temperature. The fixation solution was removed and cells were washed with PBS. Cells were permeabilized with 0.2% Triton-X in PBS and incubated for 10 min. Cells were washed with PBS and incubated with PBS containing 3% FBS for 30 min. Cells were then stained overnight at 4 °C with Phos-Histone H3 (Ser10)-Alexa Fluor 488 Conjugate antibody (Cell Signaling) solution in PBS plus 3% FBS. Cells were washed with PBS and then immunofluorescence images were captured at 10 $\times$  with HT Pathway 855 automated fluorescent microscope (BD Bioscience). Percent positive cells were quantitated using Hoechst staining for cell number using Attovision software (BD Bioscience). To generate IC<sub>50</sub> values, the dose–response curves were then fitted to a standard sigmoidal curve and IC<sub>50</sub> values were derived by nonlinear regression analysis.
16. DeLano, W. L. *The PyMOL Molecular Graphics System*; DeLano Scientific: Palo Alto, CA, 2002.
17. Sorota, S.; Zhang, X. S.; Margulis, M.; Tucker, K.; Priestley, T. *Assay Drug Dev. Technol.* **2005**, *3*, 47.